



ELSEVIER

Available online at [www.sciencedirect.com](http://www.sciencedirect.com)

SCIENCE @ DIRECT®

Journal of Sound and Vibration 272 (2004) 967–989

JOURNAL OF  
SOUND AND  
VIBRATION

[www.elsevier.com/locate/jsvi](http://www.elsevier.com/locate/jsvi)

# Estimating unbalance and misalignment of a flexible rotating machine from a single run-down

J.K. Sinha<sup>a</sup>, A.W. Lees<sup>b</sup>, M.I. Friswell<sup>c,\*</sup>

<sup>a</sup>*Vibration Laboratory, Reactor Engineering Division, BARC, Mumbai 400 085, India*

<sup>b</sup>*School of Engineering, University of Wales Swansea, Swansea SA2 8PP, UK*

<sup>c</sup>*Department of Aerospace Engineering, University of Bristol, Bristol BS8 1TR, UK*

Received 6 December 2002; accepted 24 March 2003

---

## Abstract

Earlier studies have suggested that the reliable estimation of the state of unbalance (both amplitude and phase) at multiple planes of a flexibly supported rotating machine from measured vibration data is possible using a single machine run-down. This paper proposes a method that can reliably estimate both the rotor unbalance and misalignment from a single machine run-down. This identification assumes that the source of misalignment is at the couplings of the multi-rotor system, and that this will generate constant synchronous forces and moments at the couplings depending upon the extent of the off-set between the two rotors, irrespective of the machine rotating speed. A flexible foundation model is also estimated. The method is demonstrated using experimental data from a machine with two bearings and a flexible coupling to the motor. A sensitivity analysis has also been carried out for the proposed approach with perturbation errors in the rotor and bearing models, to confirm the robustness of the method.

© 2003 Elsevier Ltd. All rights reserved.

---

## 1. Introduction

Many rotating machines, such as power station turbogenerators, may be considered as consisting of three major parts; the rotor, the bearings (often fluid bearings) and the foundations. In many modern systems, the foundation structures are flexible and have a substantial influence on the dynamic behaviour of the complete machine. These rotating machines have a high capital cost and hence the development of condition monitoring techniques is very important. Vibration-based identification of faults, such as rotor unbalance, rotor bends, cracks, rubs, misalignment,

---

\*Corresponding author. Tel.: +44-117-928-8695; fax: +44-117-927-2771.

*E-mail addresses:* [vired@magnum.barc.ernet.in](mailto:vired@magnum.barc.ernet.in) (J.K. Sinha), [a.w.lees@swansea.ac.uk](mailto:a.w.lees@swansea.ac.uk) (A.W. Lees), [m.i.friswell@bristol.ac.uk](mailto:m.i.friswell@bristol.ac.uk) (M.I. Friswell).

fluid induced instability, based on the qualitative understanding of measured data, is well-developed [1] and widely used in practice. However the quantitative part, the estimation of the extent of faults and their locations, has been an active area of research for many years. Over the past 30 years, theoretical models have played an increasing role in the rapid resolution of problems in rotating machinery. Doebling et al. [2] gave an extensive survey on the crack detection methods. Parkinson [3] and Foiles et al. [4] gave comprehensive reviews of rotor balancing. Muszynska [5] gave a thorough review of the analysis of rotor–stator rub phenomena. Edwards et al. [6] gave a brief review of the wider field of fault diagnosis. The study of the rotor misalignment has been limited to qualitative understanding of the phenomenon [7–13] but no-one has suggested a method for the direct quantification of misalignment faults.

In spite of the success of model-based estimation of faults, the construction of a reliable mathematical model of a machine on flexible foundations is still not feasible. Often a good finite element model of the rotor and an adequate model of the fluid bearing [14] may be constructed. Indeed several finite element based software packages are available for such modelling. However a reliable finite element model for the foundation is difficult, if not impossible, to construct due to a number of practical difficulties [15]. Inclusion of the foundation model is very important since the dynamics of the flexible foundation also contributes significantly to the dynamics of the complete machine. Many research studies [16–22] have been carried out to derive the foundation models directly from the measured machine responses but more research is needed on their practical application. Hence a complete mathematical model of a machine is still not available for condition monitoring in many cases.

Given the above limitations, an alternative method has been suggested by Lees and Friswell [23] for the reliable estimation of multi-plane rotor unbalance. Unbalance is one of the most frequently encountered problems in rotating machines that needs to be corrected at regular intervals with the minimum possible down time. The method of Lees and Friswell [23] has the potential for fast and reliable unbalance estimation. The method uses the measured vibration data during a single run-down (one transient operation only) of a machine, along with models of only the rotor and bearings, to estimate the multi-plane unbalance in a single step. The foundation parameters are estimated as a by-product, and hence the method also accounts for the dynamics of the foundation. Lees and Friswell [23] demonstrated the method on a simple simulated example. The method has been further validated on a small simple experimental rig [24]. In both cases the number of modes of the system were less than the measured degrees of freedom in the run-down frequency range. However in many systems, for example turbogenerator sets, the number of modes excited may be more than the measured degrees of freedom and thus the estimated unbalance may not account for all of the critical speeds. The identification method has been modified further by splitting the whole frequency range into bands so that the band-dependent foundation models account for all of the critical speeds. The advantages of the suggested approach have been demonstrated on a complex simulated example and on an experimental rig [25–27].

However, in a multi-rotor system there is always the possibility of rotor misalignment and this may influence the machine response and hence the quality of the unbalance estimation. In this paper, the method described above has been modified to estimate both the rotor unbalance and misalignment. The misalignment is assumed to affect only the rotor, whereas for systems with fluid bearings and rigidly coupled shafts the misalignment will also affect the distribution of static

loads in the fluid bearings. The general perception and observation is that misalignment in multi-coupled rotors generates a  $2\times$  (twice the rotating speed) component in the response of the machine [8,9] and the effect on the  $1\times$  component is assumed to be small. However, Jordan [28] confirms that the misalignment initially affects the  $1\times$  response resulting in an elliptical orbit, but in the case of severe misalignment the orbit plot may look like a *figure eight* due to the appearance of a  $2\times$  component in the response. These features are usually used for the detection of the presence of rotor misalignment [28]. In practice both the  $1\times$  and the  $2\times$  response will be affected by misalignment, and the physical source of these effects may be modelled as a rotor bend and rotor asymmetry, respectively. In this paper the identification of rotor unbalance and misalignment uses the  $1\times$  response at the bearing pedestals of the machine from a single run-down, even though the direct influence on the  $1\times$  response due to misalignment may be small.

Here it is assumed that the source of the rotor misalignment is the couplings of the multi-rotor system. Such a misalignment is assumed to generate constant synchronous forces and moments at the couplings depending upon the extent of the off-set between the two rotors and irrespective of the machine rotating speed [7]. The force vector in the equation of motion is assumed to consist of both the unbalance forces and the constant forces and moments at the couplings, and these parameters are estimated along with the foundation model. The method is demonstrated using experimental data from a machine with two bearings and a flexible coupling to the motor. In a real machine, accurate models of the rotor and fluid bearings may not be available. Thus a sensitivity analysis for the proposed approach has been performed, with perturbation errors in the rotor and fluid bearing models, to confirm the robustness of the method.

## 2. Theory

Fig. 1 shows the abstract representation of a rotating machine, where a rotor is connected to a flexible foundation via flexible bearings. The equations of motion of the system may be written

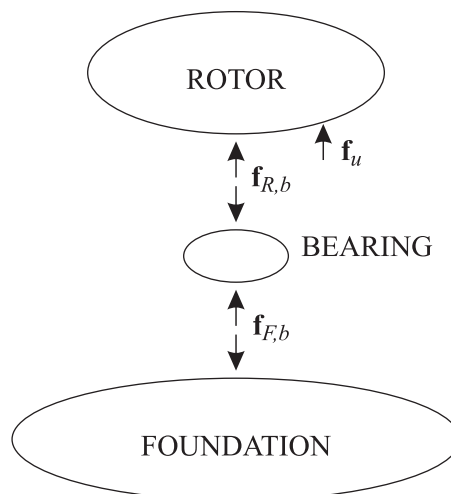


Fig. 1. The abstract representation of a rotating machine.

[1,26] as

$$\begin{bmatrix} \mathbf{Z}_{R,ii} & \mathbf{Z}_{R,ib} & \mathbf{0} \\ \mathbf{Z}_{R,bi} & \mathbf{Z}_{R,bb} + \mathbf{Z}_B & -\mathbf{Z}_B \\ \mathbf{0} & -\mathbf{Z}_B & \mathbf{Z}_B + \bar{\mathbf{Z}}_F \end{bmatrix} \begin{Bmatrix} \mathbf{r}_{R,i} \\ \mathbf{r}_{R,b} \\ \mathbf{r}_{F,b} \end{Bmatrix} = \begin{Bmatrix} \mathbf{f}_u \\ \mathbf{0} \\ \mathbf{0} \end{Bmatrix}, \tag{1}$$

where  $\mathbf{Z}$  is the dynamic stiffness matrix, the subscripts  $i$  and  $b$  refer to internal and bearing (connection) degrees of freedom, respectively, and the subscripts  $F, R,$  and  $B$  refer to the foundation, the rotor and the bearings.  $\mathbf{r}$  are the responses and  $\mathbf{f}_u$  are the force vectors, which are assumed to be applied only at the rotor internal degrees of freedom. The dynamic stiffness matrix of the foundation,  $\bar{\mathbf{Z}}_F$ , is defined only at the degrees of freedom connecting the bearings and the foundation. In practice this will be a reduced order model, where the internal foundation degrees of freedom have been eliminated [1]. The dynamic stiffness matrix of the bearings is given by  $\mathbf{Z}_B$ . It has been assumed that the inertia effects within the bearings are negligible, although these could be included if required.

Solving Eq. (1) to eliminate the unknown response of the rotor gives

$$\bar{\mathbf{Z}}_F \mathbf{r}_{F,b} = \mathbf{Z}_B (\mathbf{P}^{-1} \mathbf{Z}_B - \mathbf{I}) \mathbf{r}_{F,b} - \mathbf{Z}_B \mathbf{P}^{-1} \mathbf{Z}_{R,bi} \mathbf{Z}_{R,ii}^{-1} \mathbf{f}_u, \tag{2}$$

where  $\mathbf{P} = \mathbf{Z}_{R,bb} + \mathbf{Z}_B - \mathbf{Z}_{R,bi} \mathbf{Z}_{R,ii}^{-1} \mathbf{Z}_{R,ib}$ . It is assumed that good models for the rotor and the bearings,  $\mathbf{Z}_R$  and  $\mathbf{Z}_B$ , are known a priori and  $\mathbf{r}_{F,b}$  is the vector of measured responses during a single run-down of a machine. Thus, the only unknown quantities in Eq. (2) are the foundation model,  $\bar{\mathbf{Z}}_F$ , and the force vector,  $\mathbf{f}_u$ . The force vector may be defined as

$$\mathbf{f}_u = \mathbf{f}_{um} + \mathbf{f}_m, \tag{3}$$

where  $\mathbf{f}_{um}$  is the vector of unbalance forces and  $\mathbf{f}_m$  is the vector of forces and moments at the couplings.

### 2.1. Modelling unbalance forces

Although the unbalance will be distributed throughout the rotor, this is equivalent to a discrete distribution of unbalance, provided there are as many balance planes as active modes. Suppose the unbalance planes are located at nodes  $n_1, n_2, \dots, n_p$ , where  $p$  is the number of planes. The associated amplitude of unbalance (defined as the unbalance mass multiplied by distance between the mass and geometric centres) and phase angles are  $[u_{n_1}, u_{n_2}, \dots, u_{n_p}]^T$  and  $[\theta_{n_1}, \theta_{n_2}, \dots, \theta_{n_p}]^T$ , respectively. These amplitudes and phase angles can be expressed, for the  $i$ th balance plane, as the complex quantity  $u_{n_i} \exp(j\theta_{n_i}) = e_{r,n_i} + j e_{i,n_i}$ . Hence, the unbalance forces,  $\mathbf{f}_{um}$ , in the horizontal and vertical directions, can be written as [1,26]

$$\mathbf{f}_{um} = \omega^2 \mathbf{T} \mathbf{e}, \tag{4}$$

where  $\mathbf{e} = [e_{r,n_1} e_{r,n_2} \dots e_{r,n_p} e_{i,n_1} e_{i,n_2} \dots e_{i,n_p}]^T$  and  $\mathbf{T}$  is a selection matrix indicating the location of the balance planes.

### 2.2. Modelling misalignment forces and moments

It has been assumed that the rotor misalignment occurs at the couplings between the multi-rotors. The nature of the rotor misalignment could be parallel, angular or combined as shown in

Fig. 2, but all of them would generate forces and/or moments. Suppose that there are  $c$  couplings in the rotor located at nodes  $m_1, m_2, \dots, m_c$ . The associated amplitude of the forces and moments are  $\mathbf{e}_m = [f_{z,m_1} \ f_{y,m_1} \ M_{y,m_1} \ M_{z,m_1} \ f_{z,m_2} \ f_{y,m_2} \ \dots \ f_{z,m_c} \ f_{y,m_c} \ M_{y,m_c} \ M_{z,m_c}]^T$ , where the subscripts  $y$  and  $z$  represent the horizontal and vertical directions and  $f$  and  $M$  are forces and moments, respectively. Hence, the misalignment force,  $\mathbf{f}_m$ , can be written as [1]

$$\mathbf{f}_m = \mathbf{T}_m \mathbf{e}_m, \tag{5}$$

where  $\mathbf{T}_m$  is the transformation matrix indicating the location of the couplings [1].

The proposed method will estimate the forces and moments due to the rotor misalignment. However, it is often more intuitive to consider displacements and angles rather than forces and moments, although this requires the stiffness matrix of the coupling. Suppose that the stiffness of the  $i$ th coupling is  $\mathbf{K}_{c,i}$ , then the linear misalignment,  $\Delta y_i$  and  $\Delta z_i$ , and the angular misalignment,  $\Delta\theta_{y,i}$  and  $\Delta\theta_{z,i}$ , at the  $i$ th coupling in the horizontal and the vertical directions may be calculated as [1]

$$\begin{Bmatrix} \Delta z_i \\ \Delta y_i \\ \Delta\theta_{y,i} \\ \Delta\theta_{z,i} \end{Bmatrix} = [\mathbf{K}_{c,i}]^{-1} \begin{Bmatrix} f_{z,i} \\ f_{y,i} \\ M_{y,i} \\ M_{z,i} \end{Bmatrix}. \tag{6}$$

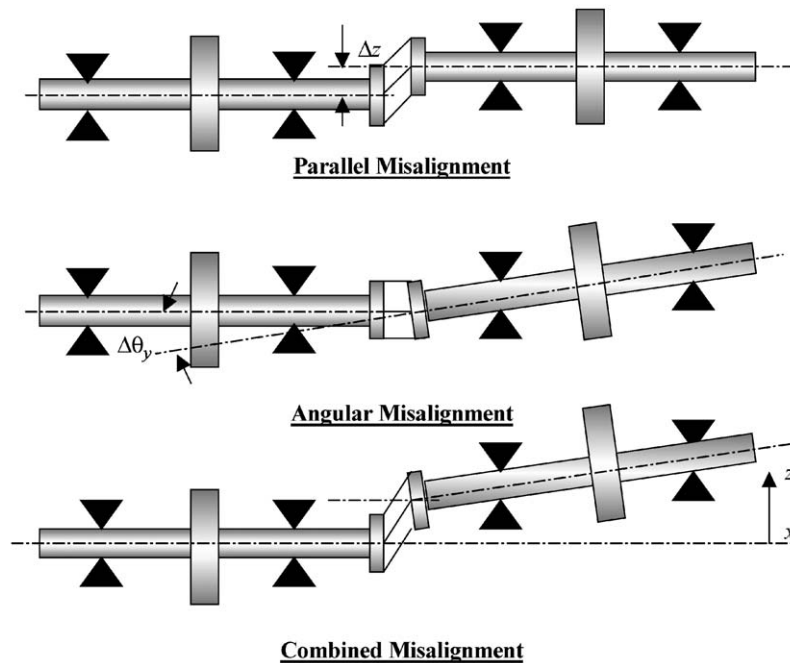


Fig. 2. Schematic of rotor with misalignment at a coupling.

2.3. *Parameter estimation*

Substituting Eqs. (4) and (5) into Eq. (2) produces

$$\bar{\mathbf{Z}}_F \mathbf{r}_{F,b} + \mathbf{Z}_B \mathbf{P}^{-1} \mathbf{Z}_{R,bi} \mathbf{Z}_{R,ii}^{-1} [\omega^2 \mathbf{T} \quad \mathbf{T}_m] \begin{Bmatrix} \mathbf{e} \\ \mathbf{e}_m \end{Bmatrix} = \mathbf{Z}_B [\mathbf{P}^{-1} \mathbf{Z}_B - \mathbf{I}] \mathbf{r}_{F,b}. \tag{7}$$

To identify the foundation parameters and forces in a least-squares sense, the foundation parameters are grouped into a vector  $\mathbf{v}$ . Suppose that the foundation dynamic stiffness matrix,  $\bar{\mathbf{Z}}_F$ , is written in terms of mass, damping and stiffness matrices. If there are  $n$  measured degrees-of-freedom at the foundation-bearing interface, then  $\mathbf{v}$  will take the form

$$\mathbf{v} = [\bar{k}_{F,11} \quad \bar{k}_{F,12} \quad \cdots \quad \bar{k}_{F,m} \quad \bar{c}_{F,11} \quad \bar{c}_{F,12} \quad \cdots \quad \bar{c}_{F,m} \quad \bar{m}_{F,11} \quad \bar{m}_{F,12} \quad \cdots \quad \bar{m}_{F,m}]^T, \tag{8}$$

where the elements in  $\mathbf{v}$  are individual elements of the structural matrices. With this definition of  $\mathbf{v}$ , there is a linear transformation such that

$$\bar{\mathbf{Z}}_F \mathbf{r}_{F,b} = \mathbf{W} \mathbf{v}, \tag{9}$$

where  $\mathbf{W}$  contains the response terms at each measured frequency [1]. For the  $q$ th measured frequency

$$\mathbf{W}(\omega_q) = [\mathbf{W}_0(\omega_q) \quad \mathbf{W}_1(\omega_q) \quad \mathbf{W}_2(\omega_q)], \tag{10}$$

where, if all elements of the foundation mass, damping and stiffness matrices are identified,

$$\mathbf{W}_k(\omega_q) = (j\omega_q)^k \begin{bmatrix} \mathbf{r}_{F,b}^T(\omega_q) & \mathbf{0} & \cdots & \mathbf{0} \\ \mathbf{0} & \mathbf{r}_{F,b}^T(\omega_q) & & \mathbf{0} \\ \vdots & \vdots & \ddots & \vdots \\ \mathbf{0} & \mathbf{0} & \cdots & \mathbf{r}_{F,b}^T(\omega_q) \end{bmatrix}, \tag{11}$$

for  $k = 0, 1, 2$ . Eq. (7) then becomes

$$[\mathbf{W}(\omega_q) \quad \mathbf{R}(\omega_q) \quad \mathbf{R}_m(\omega_q)] \begin{Bmatrix} \mathbf{v} \\ \mathbf{e} \\ \mathbf{e}_m \end{Bmatrix} = \mathbf{Q}(\omega_q), \tag{12}$$

where the form of  $\mathbf{R}$ ,  $\mathbf{R}_m$  and  $\mathbf{Q}$  may be obtained by comparing Eqs. (7), (11) and (12), as

$$\mathbf{R}(\omega_q) = \omega_q^2 \mathbf{Z}_B(\omega_q) \mathbf{P}^{-1}(\omega_q) \mathbf{Z}_{R,bi}(\omega_q) \mathbf{Z}_{R,ii}^{-1}(\omega_q) \mathbf{T}, \tag{13}$$

$$\mathbf{Q}(\omega_q) = \mathbf{Z}_B(\omega_q) [\mathbf{P}^{-1}(\omega_q) \mathbf{Z}_B(\omega_q) - \mathbf{I}] \mathbf{r}_{F,b}(\omega_q), \tag{14}$$

$$\mathbf{R}_m(\omega_q) = \mathbf{Z}_B(\omega_q) \mathbf{P}^{-1}(\omega_q) \mathbf{Z}_{R,bi}(\omega_q) \mathbf{Z}_{R,ii}^{-1}(\omega_q) \mathbf{T}_m. \tag{15}$$

Clearly there is an equation of the form of Eq. (12) at every frequency. The equations generated may be solved in a least-squares sense directly, although the solution via the singular value decomposition (SVD) is more robust. Such an equation error approach does not optimize the error in the response directly, and thus the accuracy of the predicted response is not assured. The great advantage is that the equations are linear in the parameters. However a non-linear optimization (output error) may be performed, starting with linear estimated parameters, if a

more accurate prediction of the response is required [1,22]. In the present paper, only the equation error approach has been considered in order to concentrate on the influence of frequency range subdivision. Furthermore, the unbalance and misalignment seems to be estimated robustly by the equation error approach, even if the foundation is relatively inaccurate [24].

### 2.4. Splitting the frequency range

The number of degrees-of-freedom of the foundation model estimated by the above method would be equal to the number of measurement locations during the machine run-down. Often, especially for large machines, the number of critical speeds of the system in the run-down frequency range, is more than the number of measurement locations. This requires splitting the entire frequency range into smaller bands and the foundation models have to be estimated for each frequency band [22,26]. The splitting of the frequency range may be performed by a visual inspection of the measured responses, together with some experience and a trial and error approach. However, the first trial itself will give a good estimate if the number of frequency peaks seen on the measured responses (both in the vertical and horizontal directions) are less than the total number of degrees-of-freedom of the foundation model to be estimated in each frequency band.

Suppose that the frequencies at which the response is measured are  $\omega_q, q = 1, \dots, N$ . Assume that the run-down frequency range is split into  $b$  frequency bands. The vectors of the foundation parameters are identified in each frequency band, and are denoted  $\mathbf{v}_1, \mathbf{v}_2, \dots, \mathbf{v}_b$ . Hence combining the frequency-band-dependent foundation models and the global unbalance and misalignment, in a similar way to the unbalance estimation [26], gives, from Eq. (12)

$$\begin{bmatrix} \mathbf{W}_{band\_1} & \mathbf{0} & \cdots & \mathbf{0} & \mathbf{R}_{band\_1} & \mathbf{R}_{m,band\_1} \\ \mathbf{0} & \mathbf{W}_{band\_2} & \cdots & \mathbf{0} & \mathbf{R}_{band\_2} & \mathbf{R}_{m,band\_2} \\ \vdots & \vdots & \ddots & \vdots & \vdots & \vdots \\ \mathbf{0} & \mathbf{0} & \cdots & \mathbf{W}_{band\_b} & \mathbf{R}_{band\_b} & \mathbf{R}_{m,band\_b} \end{bmatrix} \begin{Bmatrix} \mathbf{v}_1 \\ \mathbf{v}_2 \\ \vdots \\ \mathbf{v}_b \\ \mathbf{e} \\ \mathbf{e}_m \end{Bmatrix} = \begin{Bmatrix} \mathbf{Q}_{band\_1} \\ \mathbf{Q}_{band\_2} \\ \vdots \\ \mathbf{Q}_{band\_b} \end{Bmatrix}. \quad (16)$$

### 2.5. Regularization

Eq. (16) is a least-squares problem, and its solution is likely to be ill conditioned [1,26]. The following three types of *regularization* were used to solve the least-squares problem.

#### 2.5.1. Regularization Method 1

In solving the least-squares problem, generally two types of scaling, namely row scaling and column scaling, may be applied [29]. Column scaling is necessary because of the different magnitudes of elements of the  $\bar{\mathbf{M}}_F, \bar{\mathbf{C}}_F$  and  $\bar{\mathbf{K}}_F$  matrices, and the scaling factors used here were 1,  $\bar{\omega}$  and  $\bar{\omega}^2$  respectively, where  $\bar{\omega}$  is the mean value of the frequency range. The scaling of the columns of  $\mathbf{R}$  and  $\mathbf{R}_m$  depend upon engineering judgement based on the unbalance and misalignment magnitudes expected. Truncated SVD was used to solve the equations [30].

### 2.5.2. Regularization Method 2

Other physically based constraints may be applied to the foundation model to improve the conditioning in addition to *Regularization Method 1*. For example, the mass, damping and stiffness matrices of the foundation may be assumed to be symmetric, therefore reducing the number of unknown foundation parameters. Other constraints could be introduced, such as a diagonal mass or damping matrix, or block diagonal matrices if bearing pedestals do not interact dynamically.

Depending upon the physical constraints applied to the foundation model, the vector  $\mathbf{v}_\ell^*$  of the foundation parameters to be estimated in each frequency band may be defined as

$$\mathbf{v}_\ell = \mathbf{T}_\ell^* \mathbf{v}_\ell^*, \quad (17)$$

where  $\ell = 1, 2, \dots, b$  and  $\mathbf{T}_\ell^*$  are the transformation matrices. Substituting Eq. (17) into Eq. (16) produces an equivalent set of equations for the unknown parameters, with the important difference that the number of parameters to be estimated is reduced. This will improve the conditioning of the estimation problem at the expense of a larger residual in the fitted equation.

### 2.5.3. Regularization Method 3

The partitioning of the system dynamic matrices in Eq. (1) includes the sub-matrix  $\mathbf{Z}_{R,ii}$ , which is the dynamic matrix of the rotor where the degrees-of-freedom at the bearing locations have been fixed (that is the rotor is pinned at the bearings). The estimation equations require that this sub-matrix be inverted and this will clearly lead to problems near the natural frequencies of the rotor with pinned supports, where the matrix  $\mathbf{Z}_{R,ii}$  would be close to singular. This ill-conditioning is particularly bad for lightly damped rotors, and the errors introduced result in meaningless parameter estimates. The approach adopted in this paper is to remove the run-down data within a small frequency band close to these problem frequencies.

## 3. Experimental example: the small rig

Fig. 3 shows a photograph of the experimental rig installed in the Dynamics Laboratory at the University of Wales Swansea (UK). Each foundation of this rig consists of a horizontal beam (500 mm × 25.5 mm × 6.4 mm) and a vertical beam (322 mm × 25.5 mm × 6.4 mm) made of steel. The horizontal beam is bolted to the base plate and the vertical beam to the bearing assembly as seen in the photograph. A layer of acrylic foam (315 mm × 19 mm × 1 mm) was bonded to the vertical beam and thin layers of metal sheet (315 mm × 19 mm × 350 μm) added to increase the damping. Modal testing confirms that the damping of the foundation increased from 0.6% to 1.4% for the first lateral mode, due to this damping layer. A 12 mm outside diameter ( $d$ ) steel shaft of 980 mm length is connected to these flexible supports and is coupled to the motor through a flexible coupling. The Young's modulus of elasticity and the density of shaft material are 200 GN/m<sup>2</sup> and 7800 kg/m<sup>3</sup>, respectively. The translational stiffness ( $k_t$ ) and rotational stiffness ( $k_\theta$ ) of the flexible coupling are estimated to be 27 kN/m and 25 Nm/rad, respectively [1]. One flexible foundation is connected at 15 mm and another at 765 mm from the right end of the shaft through self-lubricating ball bearings. The shaft also carries two identical balancing disks of



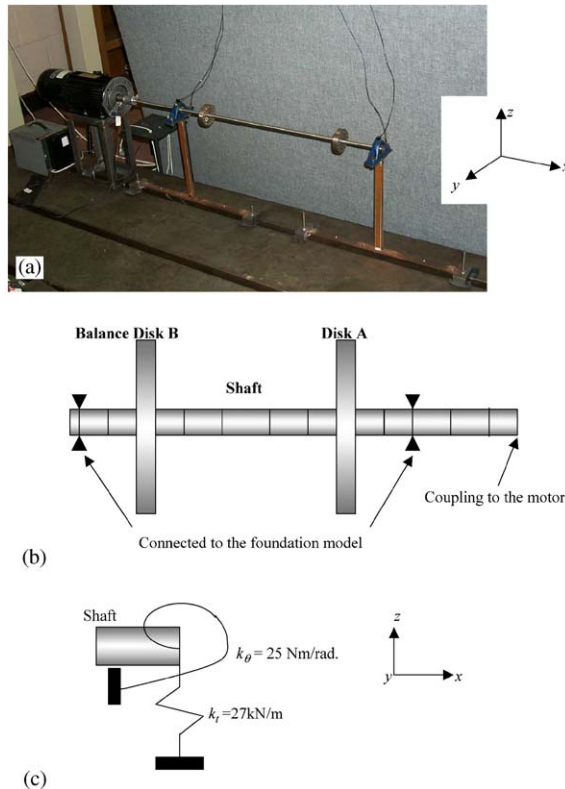


Fig. 3. The small rig at the University of Wales Swansea (UK). (a) Photograph of the small rig (b) FE model of the rotor (c) Modelling of the coupling stiffness in  $x$ - $z$  plane.

75 mm outside diameter and 15 mm thickness and placed at 140 and 640 mm from the right end of the shaft. Disk A is defined as the one nearest to the motor.

### 3.1. Run-down experiments

Different run-down experiments were performed with the rotor speed reducing from 2500 r.p.m. to 300 r.p.m. for different combinations of added mass to the balance disks A and B listed in Table 1. Runs 1 and 4 were residual run-downs, i.e., without any added mass to the disks. Order tracking was performed using the VSI Rotate software [31] such that each set of the run-down data consisted of the  $1 \times$  component of the displacement responses in the frequency range from 5.094 to 40.969 Hz in steps of 0.125 Hz.

### 3.2. Rotor unbalance and misalignment estimation

A finite element model was created for the rotor using two-noded Euler–Bernoulli beam elements, each with two translational and two rotational degrees of freedom. The finite element model of the rotor is shown in Fig. 3(b) and the modelling details of the flexible coupling in  $x$ - $z$

Table 1

Estimation of both the rotor unbalance and misalignment from the experimental run-down data for the small rig

Run	Disk	Actual unbalance (g at deg.)	Estimated unbalance (g at deg.)	Estimated misalignment				Added unbalance (g at deg.)	
				Hori., $\Delta y$ (mm)	Vert., $\Delta z$ (mm)	Hori. angle $\Delta\theta_z$ (deg.)	Ver. angle $\Delta\theta_y$ (deg.)	With respect to run 1	With respect to run 4
1	A	Residual	1.84 at 130	0.10	0.21	0.40	0.69	—	—
	B	Residual	1.46 at 350						
4	A	Residual	1.99 at 127	0.09	0.18	0.32	0.20	—	—
	B	Residual	1.44 at 341						
2	A	0.76 at 180	2.48 at 144	0.14	0.20	0.75	0.45	0.82 at 181	0.82 at 190
	B	0.76 at 0	2.33 at 354					0.88 at -4	0.98 at 14
3	A	1.52 at 180	2.75 at 158	0.14	0.18	0.42	0.16	1.41 at 191	1.46 at 202
	B	1.52 at 0	2.96 at 1					1.55 at 11	1.67 at 18
5	A	0.76 at 45	2.54 at 114	0.08	0.21	0.24	0.17	0.95 at 79	0.76 at 76
	B	0.76 at 225	1.34 at 323					0.66 at 236	0.45 at 228

plane in Fig. 3(c). Sinha [1] gave details of the dynamic characterization of the rig by modal tests and finite element analysis.

Four critical speeds (two in the horizontal and one each in the vertical and axial directions) of the machine were present in the run-down frequency range of 5.094–40.969 Hz. The unbalance and misalignment estimation was performed using the suggested method for individual runs assuming misalignment forces and moments at the coupling of the rotor with the motor. All three regularization methods were used during estimation process by assuming symmetric system matrices for the foundation parameters and the removal of a small frequency band of 1.25 Hz on either side of 38.37 Hz (the natural frequency of the rotor with pinned supports at the bearings) from the machine run-down. The frequency range was split into three bands; 5.094–12.094 Hz, 12.094–27.469 Hz, and 27.469–40.969 Hz based on the observation that the estimated responses were a close fit to the measured responses using these bands. The estimated results are listed in Table 1 and Fig. 4 compares typical measured and estimated responses.

Fig. 4 shows that the fit of the estimated response is a close fit to the measured data. Table 1 also shows that the estimated unbalance is excellent and close to the actual values and the estimated misalignment in the rotor at the coupling is quite consistent for each run. The order of the estimated misalignment (approximately 0.1 and 0.2 mm in the horizontal and vertical directions and their related angular misalignment is 0.4 and 0.2°, respectively) is very small and such a misalignment is quite possible during the rig assembly. The small deviation in the estimation may be because of noise in the measurements, however the estimation seems to be quite robust. Hence this experimental example confirms that an accurate estimation of both the rotor unbalance and misalignment is possible using measured responses from a single run-down of a machine. However, the sensitivity analysis with perturbations in the rotor model was carried out on this experimental example to check the robustness of the proposed method.

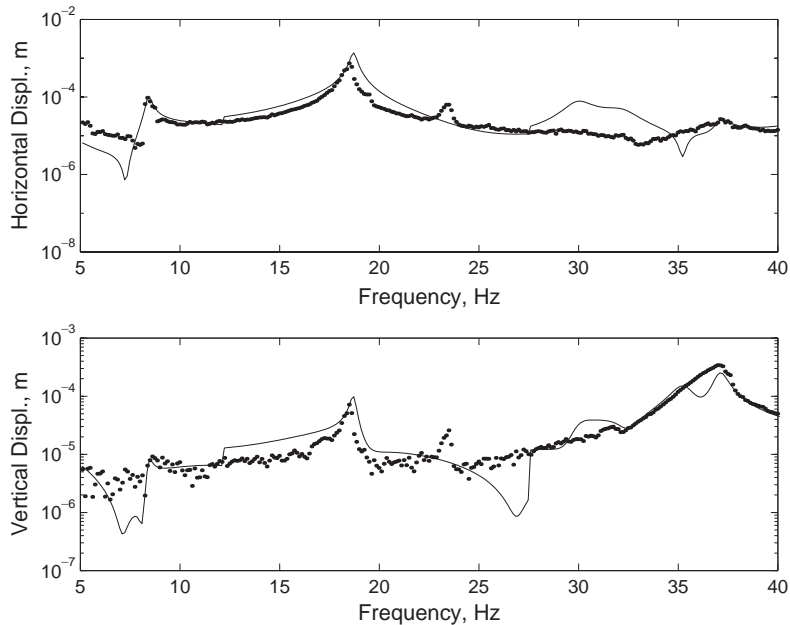


Fig. 4. Measured and estimated response at bearing A, for run 2 for the small rig (dot—measured, line—estimated).

#### 4. Sensitivity analysis

As discussed earlier, it is often difficult to get accurate values for the parameters of the rotor and fluid bearing models for rotating machines such as turbogenerator sets. Hence the estimation process was repeated with perturbations in the rotor and fluid bearing models. Initially the estimation process was repeated on the above experimental small rig example with rotor modelling errors. The estimation and sensitivity analysis was then performed on another experimental example with four fluid bearings [1,26] to give a comparison between two different types of rig.

##### 4.1. Experimental Example 1: the small rig

Fig. 3 shows the rig, which is supported by ball bearings. In the frequency range considered the bearings provide a rigid connection between the translational degrees of freedom of the rotor and the foundation at the location of the bearings. Thus no error is expected in the bearing model. Although the rotor may be modelled reasonably accurately, some small errors are expected. Here errors will be assumed in the shaft diameter ( $d$ ) and the material properties, namely the modulus of elasticity ( $E$ ) and the density ( $\rho$ ). Furthermore, the mechanical coupling stiffnesses, the translational stiffness ( $k_t$ ) and rotational stiffness ( $k_\theta$ ), are also the part of the rotor model and hence are equally important. Errors in these parameters were introduced in turn before estimating the rotor unbalance and misalignment. The errors introduced in the different parameters were  $\pm 5\%$  in shaft diameter ( $d$ ) in steps of  $0.5\%$ ,  $\pm 10\%$  in the modulus of elasticity ( $E$ ) and density ( $\rho$ ), and  $\pm 20\%$  in the coupling stiffnesses,  $k_t$  and  $k_\theta$ , in steps of  $1\%$ . Simultaneous perturbation in

all these parameters was also considered, although such a combination may be highly unlikely in practice.

The unbalance and misalignment estimates due to the perturbations in the rotor modelling parameters, for the individual experimental runs, are shown in Table 2. Fig. 5 gives a typical graphical representation of the variation in the rotor unbalance estimation from the subtracted unbalance of runs 1 and 2 (with respect to the initial estimates given in Table 1), as a function of the perturbation in individual rotor modelling parameters. For a normally distributed random perturbation error in all of the modelling parameters simultaneously, with a standard deviation of 5%, Fig. 6 shows the variation in the unbalance estimate. Figs. 5 and 6 show that the phase estimation is more robust than the unbalance amplitude. Usually the unbalance is estimated with an error of less than 40–50% with respect to the initial estimate in Table 1, except in a few cases where it is about 70–75%. Table 2 summarizes the maximum deviation in the estimated unbalance amplitudes and phases. Fig. 7 shows a typical variation in the estimates of linear and angular misalignment with the rotor modelling error for run 3. The maximum effect on the misalignment

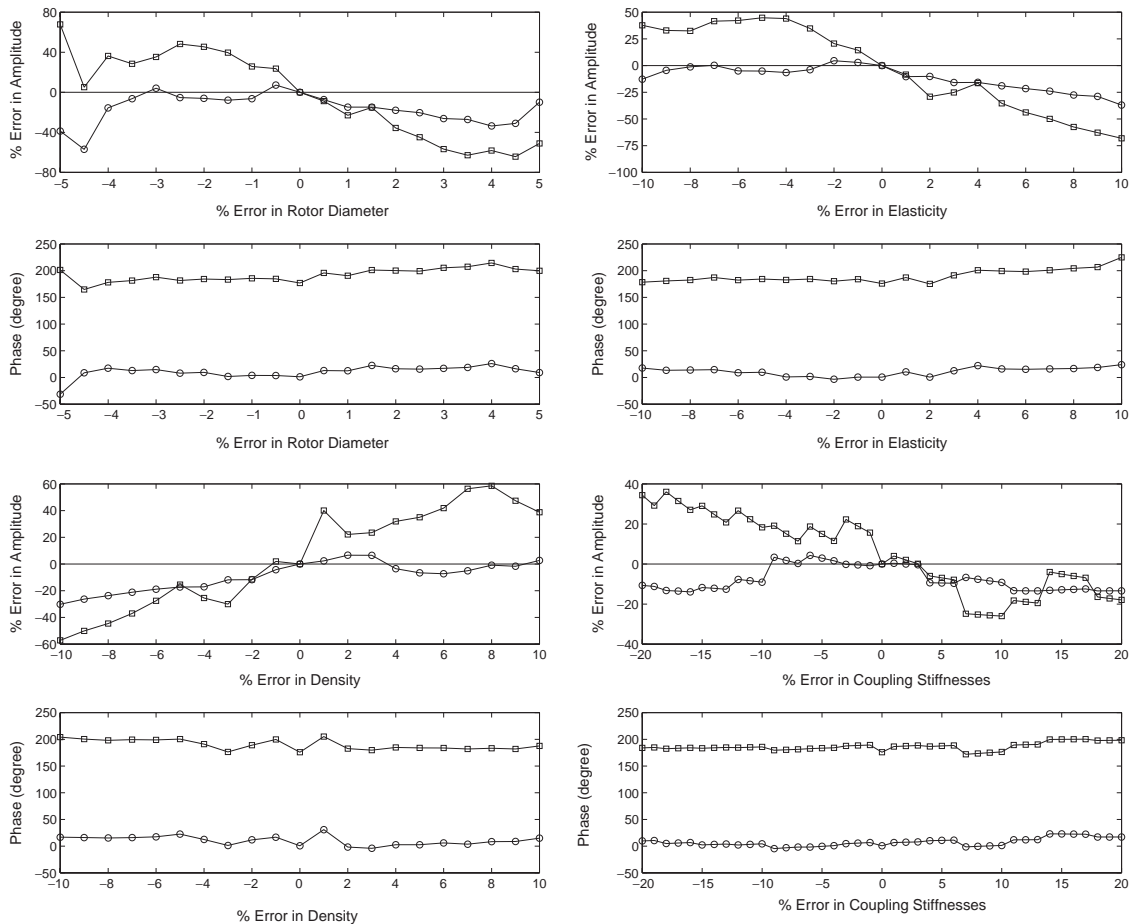


Fig. 5. Typical deviation in the rotor unbalance estimation due to errors in the rotor model of the small rig for subtracted unbalance runs 1 and 2 (square for disk A, circle for disk B).

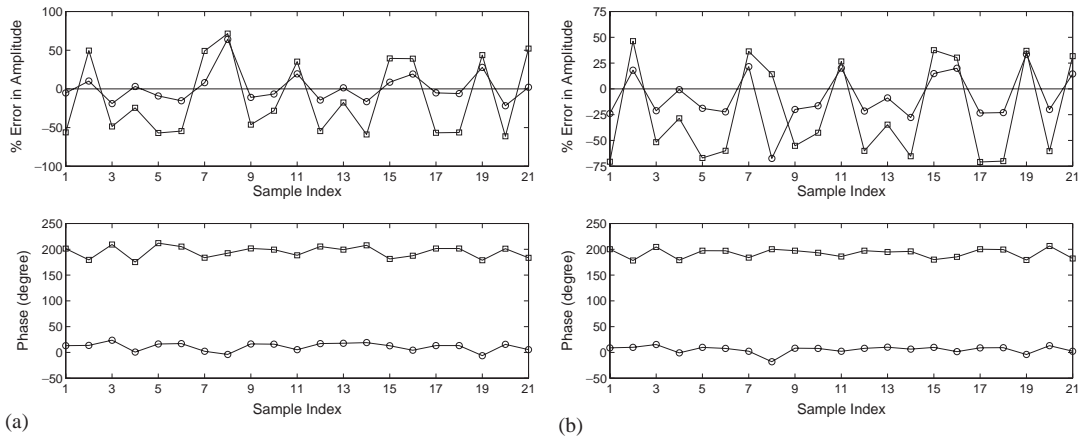


Fig. 6. Typical deviation in the rotor unbalance estimation due to 5% random errors in all rotor model parameters of the small rig (square for disk A, circle for disk B). (a) Subtracted unbalance for runs 1 & 2 (b) subtracted unbalance for runs 1 & 3.

Table 2  
Unbalance estimation for the small rig, with perturbations to the rotor model

Rotor model		Balance disk A—unbalance		Balance disk B—unbalance	
Perturbation in parameters	Error (%)	Max. % error in amplitude (%)	Max. phase error (deg.)	Max. % error in amplitude (%)	Max. phase error (deg.)
Shaft diameter ( $d$ )	$\pm 5$	70	45	60	30
Elasticity ( $E$ )	$\pm 10$	55	35	38	25
Density ( $\rho$ )	$\pm 10$	60	30	30	25
Coupl. Stiff., $k_t$ and $k_\theta$	$\pm 20$	40	20	25	25
5% Random error to all		75	20	70	20

estimation is seen when the rotor stiffness decreases by 6–10%, otherwise the variation in the estimates is small.

The above sensitivity analysis has been performed using all of the regularization methods discussed in Section 2. The effect on the estimated unbalance and misalignment of regularization methods 1 and 2 is not usually dramatic. However, the use of regularization method 3 is essential, particularly when the rotor model contains some error. Fig. 8 shows a typical example for the subtracted estimated unbalance for runs 1 and 2, as a function of the error in the rotor model, when regularization method 3 was not used. The deviation in the estimated unbalance is now very high, and demonstrates that data at the identified problem frequencies must be removed.

#### 4.2. Experimental Example 2: the Aston rig

Fig. 9 shows the test rig at Aston University, Birmingham, UK. The rig is much larger than the small rig and it consists of a solidly coupled, two-shaft system mounted on four oil lubricated journal bearings. The bearings sit on flexible steel pedestals bolted onto a large lathe bed which

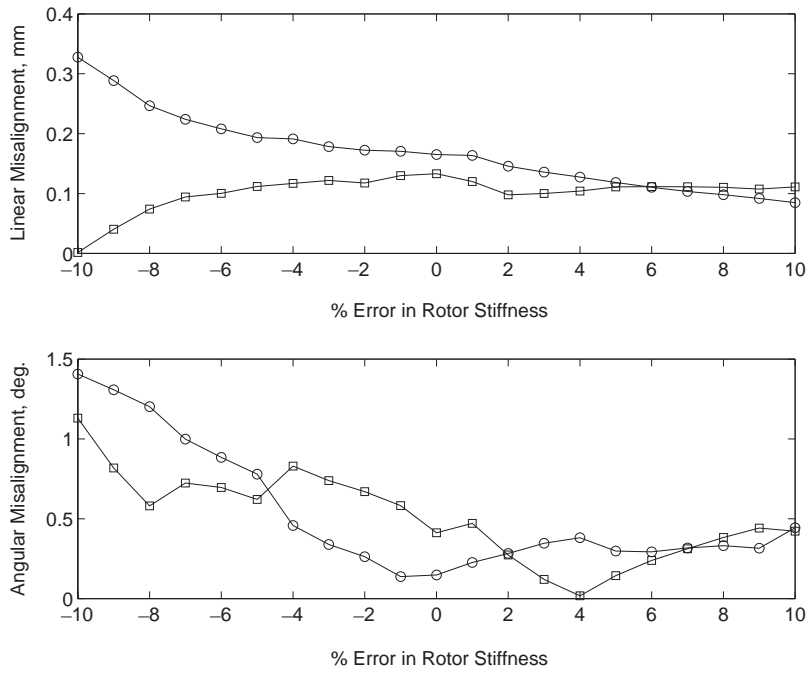


Fig. 7. Typical deviation in the rotor misalignment estimation due to errors in the rotor model of the small rig for run 3 (square for horizontal direction, circle for vertical direction).

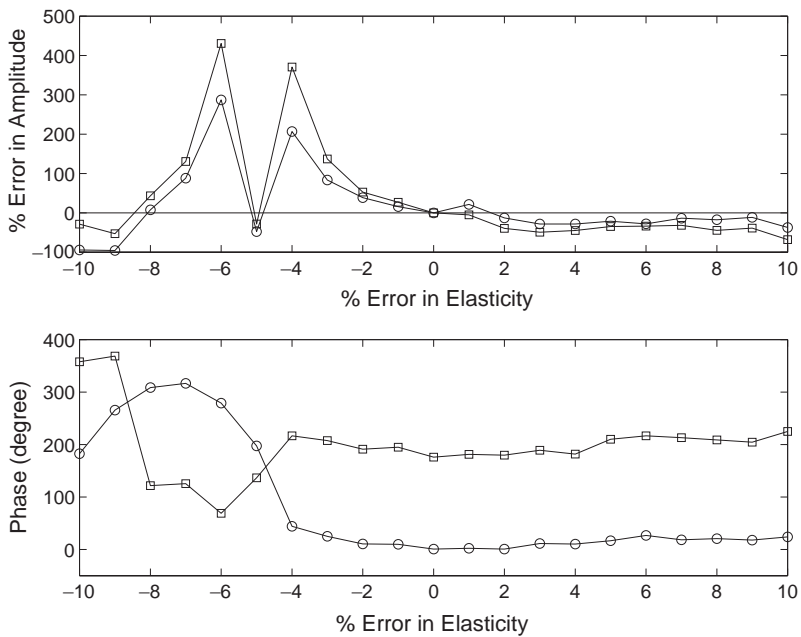


Fig. 8. Typical deviation in the rotor unbalance estimation due to errors in the rotor model of the small rig for subtracted unbalance runs 1 and 2, without regularization method 3 (square for disk A, circle for disk B).

rests on a concrete foundation. The rotor itself consists of two steel shafts 1.56 and 1.175 m long, each with a nominal diameter of 38 mm and coupled through flanges of 150 mm long and 100 mm diameter at the connecting end of both shafts. The Young's modulus of elasticity and density of the rotor material are  $200 \text{ GN/m}^2$  and  $7850 \text{ kg/m}^3$ , respectively. At either end of the shafts are journals of diameter 100 mm, and in the centre of the shafts are machined sections which take balancing disks, three for the long rotor and two for the short rotor. Each balancing disk is made of steel and is 203.2 mm in diameter and 25.4 mm thick. The balance disks were placed at 457.2, 746.8, 1016, 2351 and 2630 mm from the left end of the shaft. The dimensions of the rotor at each station are given in Table 3. The bearings are circular, have a length-to-diameter ratio of 0.3, a radial clearance of  $150 \mu\text{m}$  and contain oil of viscosity  $0.0009 \text{ Ns/m}^2$ . One bearing is located at either end of the shaft and the remaining two bearings were located at 1372 and 2046 mm from the left end. Smart [32] and Sinha et al. [26] gave a more detailed description of the rig.

Since the rig has fluid bearings the sensitivity analysis was performed for the perturbation errors in the rotor and bearing models in turn. Finally errors in both of the models simultaneously were considered and compared with the experimental example of the small rig with ball bearings. A finite element model (shown in Fig. 10) was created for the rotor with 51 two noded Timoshenko beam elements, where each node had two translational and two rotational degrees-of-freedom [1,26]. The experimental run-down responses were obtained between 55 and 5 Hz in 200 steps [1,26]. The sensitivity analysis for the unbalance estimates was performed for the subtracted experimental runs (2-1) and (3-1) listed in Table 4, which also gives the estimated unbalance with and without the use of regularization method 3 [1]. Sinha [1] and Sinha et al. [26] gave the details

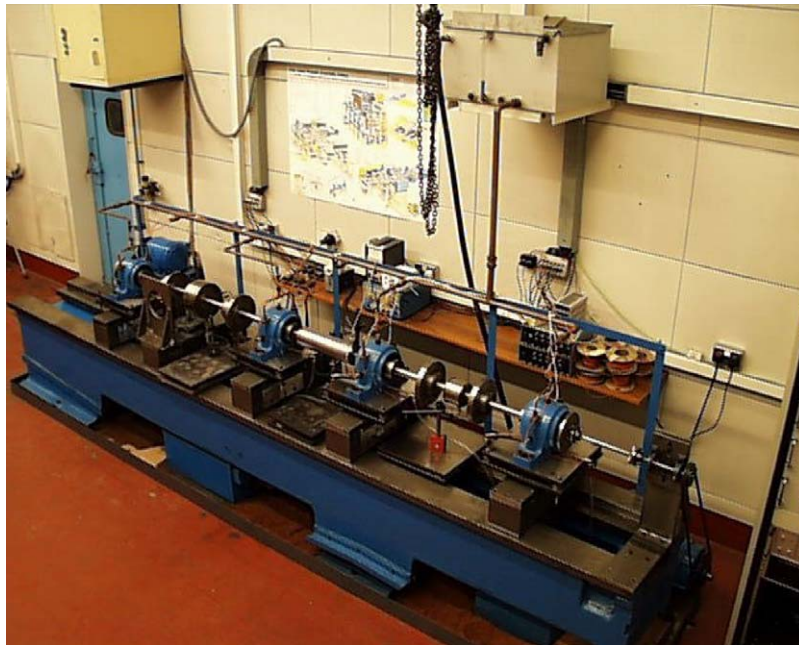


Fig. 9. Photograph of the Aston rig.

Table 3  
The physical dimensions of the rotor for the Aston rig

Long rotor properties			Short rotor properties		
Station	Length (mm)	Diameter (mm)	Station	Length (mm)	Diameter (mm)
1	203.2	100	14	6.35	38.1
2	203.2	38.1	15	25.4	77.57
3	101.6	103	16	50.8	38.1
4	177.8	38.1	17	203.2	100
5	101.6	109	18	177.8	38.1
6	177.8	38.1	19	50.8	116.8
7	101.6	117	20	76.2	38.1
8	203.2	38.1	21	76.2	109.7
9	203.2	100	22	76.2	38.1
10	50.8	38.1	23	50.8	102.9
11	25.4	78.1	24	177.8	38.1
12	12.7	38.1	25	203.2	100
13	Coupling between the two rotors through coupling flanges (see Figs. 9 and 10) of 300 mm length and 100 mm diameter				

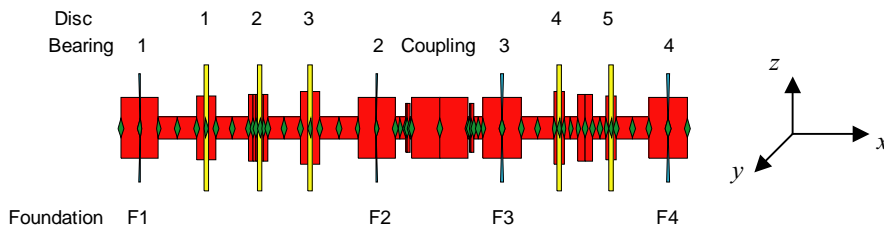


Fig. 10. Finite element model of the rotor of the Aston rig.

of the unbalance estimation for this example and these are not repeated here. Since the shaft was aligned, only unbalance estimation was considered.

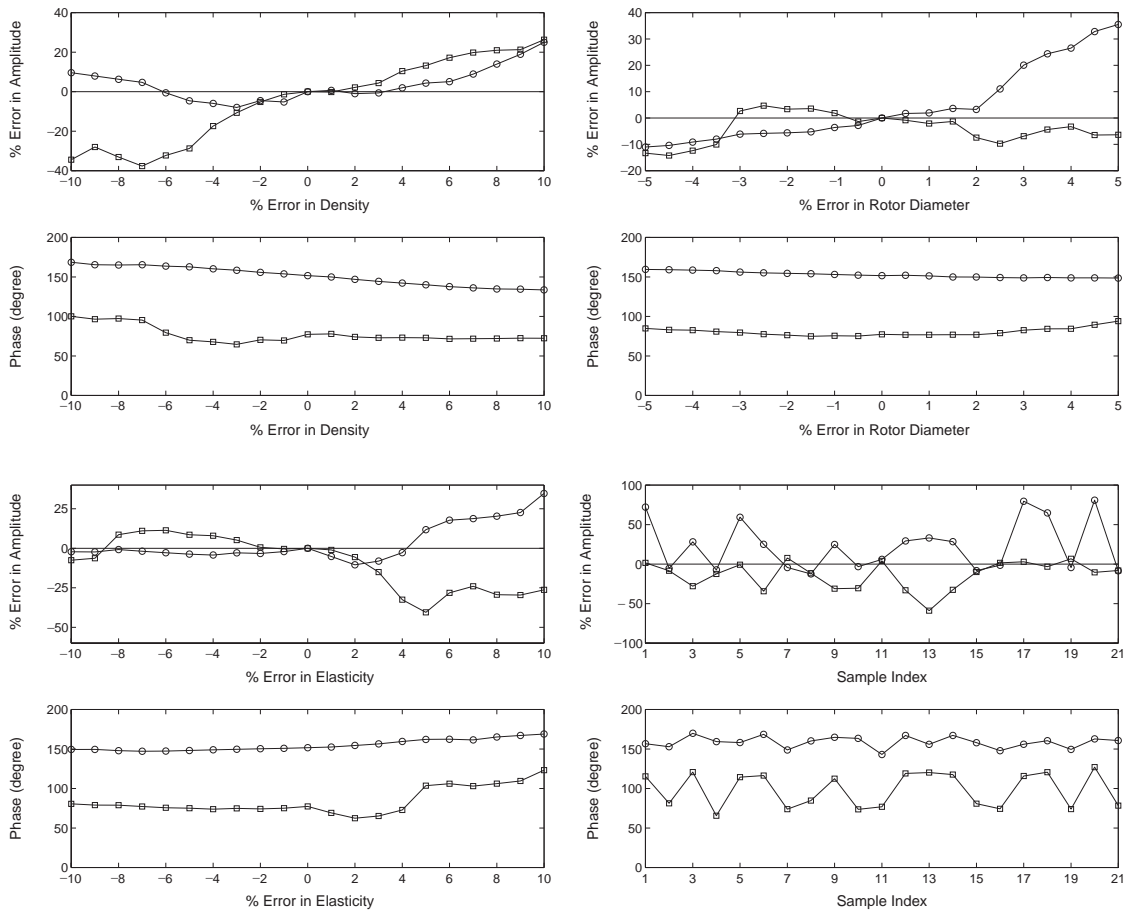
4.2.1. Error in the rotor model

Using a similar approach to the small rig example, the sensitivity analysis has been performed using perturbations in the parameters of the rotor model. Fig. 11 shows a typical graphical representation of the variation in the estimated rotor unbalance due to a perturbation in the parameters of the rotor model for run (2-1). Table 5 summarizes the maximum deviation in the estimated unbalance amplitudes and phases. Fig. 11 shows a smoother variation in the estimated unbalance amplitudes and phases, compared with the variation found in the small rig example with rigid bearings. In general the phase estimation is robust and usually invariant with the modelling error, and in some cases the estimated phase at disk 2 for run (2-1) is found to be closer to the actual phase. Although the Aston rig is much bigger than the small rig, the improved robustness to rotor modelling errors is probably because of the higher damping in the fluid bearings.



Table 4  
Unbalance estimation from the experimental run-down data by subtracting runs for the Aston rig

Run	Disk	Actual unbalance (Amplitude (g m) at phase (deg.))	Estimated unbalance (Amplitude (g m) at phase (deg.))	
			Without regularization method 3 [26,27]	With regularization method 3 [1]
2-1	2	1.7 at 105	1.529 at 51.42	1.70 at 77
	5	1.7 at 180	1.759 at 176.10	1.68 at 152
3-1	1	1.7 at 225	1.943 at 293.02	1.77 at 304
	5	1.7 at 315	1.849 at 51.40	1.65 at 48



5% random errors in all rotor parameters

Fig. 11. Typical deviation in the rotor unbalance estimation due to errors in the rotor model of the Aston rig for subtracted runs 1 and 2 (square for disk 2, circle for disk 5).

Table 5  
Unbalance estimation for the Aston rig, with perturbations to the rotor model

Rotor model		Balance disk 2—unbalance <sup>a</sup>		Balance disk 5—unbalance	
Perturbation in parameters	Error (%)	Max. % error in amplitude (%)	Max. phase error (deg.)	Max. % error in amplitude (%)	Max phase error (deg.)
<i>Run (2-1)</i>					
Shaft diameter ( $d$ )	$\pm 5$	15	15	37	10
Elasticity ( $E$ )	$\pm 10$	40	50	35	20
Density ( $\rho$ )	$\pm 10$	38	25	25	20
5% Random errors in all		60	45	80	20
<i>Run (3-1)</i>					
Shaft diameter ( $d$ )	$\pm 5$	15	7	9	5
Elasticity ( $E$ )	$\pm 10$	22	7	12	5
Density ( $\rho$ )	$\pm 10$	45	15	12	7
$\pm 5\%$ Random errors in all		45	35	20	8

<sup>a</sup> Disk 1 for run (3-1).

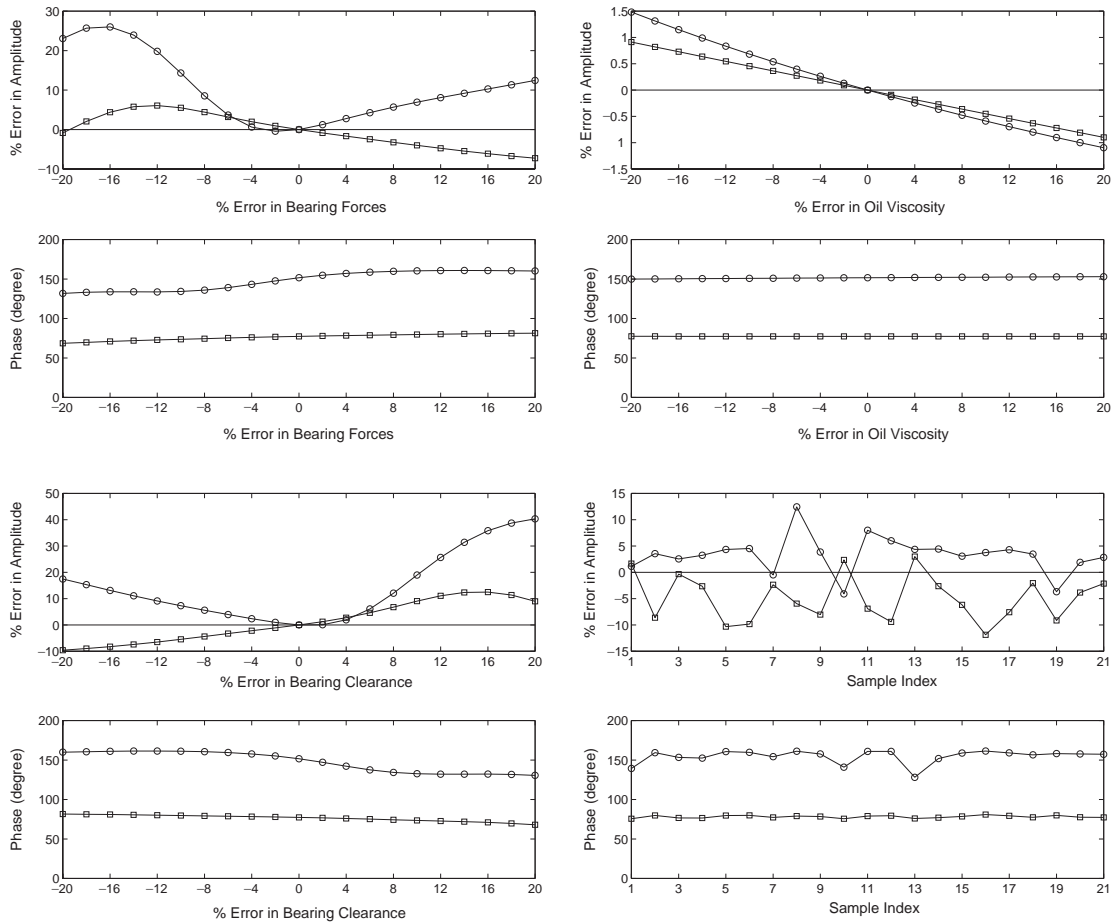
Table 6  
Unbalance estimation for the Aston rig, with perturbations to the fluid bearings model

Fluid bearing model		Balance disk 2—unbalance <sup>a</sup>		Balance disk 5—unbalance	
Perturbation in parameters	Error (%)	Max. % error in amplitude (%)	Max. phase error (deg.)	Max. % error in amplitude (%)	Max phase error (deg.)
<i>Run (2-1)</i>					
Bearing forces	$\pm 20$	6	5	27	20
Oil viscosity ( $\mu$ )	$\pm 20$	0.8	2	1.5	2
Clearance ( $\epsilon$ )	$\pm 20$	12	7	40	20
10% Random errors in all		12	3	12	20
<i>Run (3-1)</i>					
Bearing forces	$\pm 20$	12	7	17	5
Oil viscosity ( $\mu$ )	$\pm 20$	1.8	10	1.8	5
Clearance ( $\epsilon$ )	$\pm 20$	26	25	22	10
10% Random errors in all		8	20	13	20

<sup>a</sup> Disk 1 for run (3-1).

#### 4.2.2. Error in the fluid bearing model

Short bearing theory was used to model the fluid bearings, and although this theory is reasonably accurate [25–27], the model depends on the bearing static load, bearing clearance and oil viscosity [14]. The effect of errors in these parameters on the unbalance estimates was examined, by introducing the errors one at a time. First, identical variations in the parameters were assumed for all of the bearings in the machine. Second, random perturbations to all of the bearing parameters were applied. Table 6 gives the summary of the results and Fig. 12 shows typical graphical representations. The following observations may be made.



10% random errors in all parameters

Fig. 12. Typical deviation in the rotor unbalance estimation due to errors in the fluid bearing model for subtracted runs 1 and 2 for the Aston rig (square for disk 2, circle for disk 5).

- (1) The unbalance estimates are not sensitive to the bearing oil viscosity.
- (2) Bearing static load and the bearing clearance have some effect on the unbalance amplitude estimation; however, the phase estimation is once again quite robust and the error is always less than  $20^\circ$ .
- (3) In general, the errors in the unbalance estimates due to errors in the fluid bearing model are less than those due to errors in the rotor model.

Hence this study indicates that the estimation of rotor unbalance can accommodate more error in the fluid bearing models than in the rotor model.

4.2.3. Error in both the rotor and fluid bearing models

Perturbations in both the rotor and bearing models were introduced simultaneously. A normally distributed random variation was used for all of the modelling parameters with a 10%

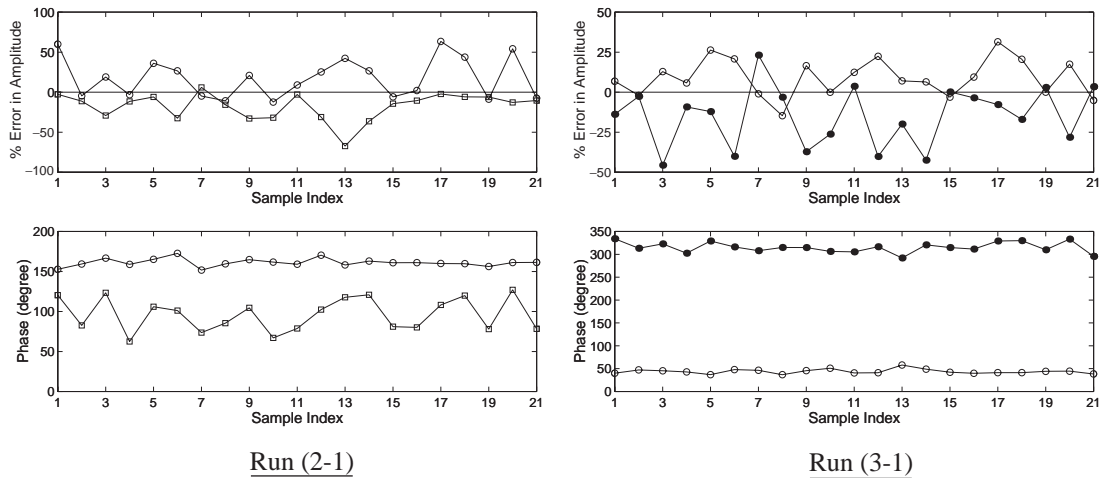


Fig. 13. Deviation in the rotor unbalance estimation due to random errors in both the rotor and the fluid bearing models for the Aston rig (dot for disk 1, square for disk 2, circle for disk 5).

standard deviation for the fluid bearing parameters and a 5% standard deviation for the rotor model parameter. Fig. 13 shows the rotor unbalance estimated for a small number of samples. The error in the estimated unbalance amplitudes is usually less than 45% except for some combinations of parameters for run (2-1) when the error is up to 70%. However the phase estimation is robust and the maximum phase error is found to be  $40^\circ$ . It should be emphasized that the combinations of errors in the parameters are unlikely to occur in practice.

## 5. Conclusions

A method to estimate both the rotor unbalance (amplitude and phase) and the misalignment of a rotor–bearing–foundation system has been presented. The estimation uses a priori rotor and bearing models along with measured vibration data at the bearing pedestals from a single run-down or run-up of the machine. The method also estimates the frequency-band-dependent foundation parameters to account for the dynamics of the foundation. The suggested method has been applied to a small experimental rig and the estimated results were excellent.

A sensitivity analysis for rotor unbalance and misalignment estimation was performed by introducing errors in the parameters of the rotor and fluid bearing models, to check the robustness of the proposed method. It has been observed that the maximum error in estimated unbalance amplitude is usually less than 45% for simultaneous random errors of 5% in the rotor model and 10% in the fluid bearing models. However, the phase estimation is quite robust which is very promising for practical rotor balancing. In practice, the authors consider that the errors in the rotor model should be much less than 5% for many machines. The variation in the estimated linear and angular misalignment due to errors in the rotor modelling was also found to be small for the small rig. In general it has been observed that the estimation method is far less sensitive to errors in the fluid bearing modelling compared to the rotor modelling error, and rotor systems

having fluid bearings are also less sensitive to modelling errors, compared to systems having rigid bearings. The importance of regularization method 3, which eliminates data near the natural frequencies of the rotor on pinned supports, has also been demonstrated. Hence the proposed method seems to be robust and gives reliable estimates of the rotor unbalance and misalignment.

### Acknowledgements

The authors acknowledge the support of the EPSRC through grant GR/M52939. Jyoti K. Sinha acknowledges Mr R. K. Sinha, Associate Director, RD & DG of his parent organization B.A.R.C., India for his consistent support and encouragement. Prof. Friswell acknowledges the support of the Royal Society as a Royal Society-Wolfson Research Merit Award holder. The assistance of Prof. John Penny and Andrew Glendenning in obtaining the measured data for the Aston rig is gratefully acknowledged.

### Appendix A. Nomenclature

<b>K, C, M</b>	stiffness, damping and mass matrices
<b>Z</b>	dynamic stiffness matrix, $-\omega^2\mathbf{M} + j\omega\mathbf{C} + \mathbf{K}$
<b>e</b>	vector of the rotor unbalance parameters
<b>e<sub>m</sub></b>	vector of the forces and moments at the couplings in multi-rotors
<b>f<sub>un</sub></b>	rotor unbalance force
<b>f<sub>m</sub></b>	rotor misalignment force
<b>j</b>	unit imaginary, $\sqrt{-1}$
<b>r</b>	responses of a machine
<b>r<sub>F,b</sub></b>	responses at the foundation connected to bearing degrees-of-freedom i.e., at the bearing pedestals
<b>T, T*, T<sub>m</sub></b>	transformation matrices for forcing degrees-of-freedom
<b>v, v*</b>	vectors of the foundation parameters
<b>x, y, z</b>	rotor axes, horizontal and vertical directions
<b>ω</b>	rotor running speed in rad/s
<b>Δy, Δz</b>	Horizontal and vertical linear misalignment at a coupling in multi-rotors (mm)
<b>Δθ<sub>y</sub>, Δθ<sub>z</sub></b>	Angular misalignment at a coupling in multi-rotors in the horizontal and vertical directions (degrees)

### Subscripts

**R, B, F** rotor, bearing, foundation

### References

- [1] J.K. Sinha, Health Monitoring Techniques for Rotating Machinery, Ph.D. Thesis, University of Wales Swansea, Swansea, 2002.

- [2] S.W. Doebling, C.R. Farrar, M.B. Prime, A summary review of vibration-based damage identification methods, *Shock and Vibration Digest* 30 (1998) 91–105.
- [3] A.G. Parkinson, Balancing of rotating machinery, *IMEchE Proceedings C—Journal of Mechanical Engineering Science* 205 (1991) 53–66.
- [4] W.C. Foiles, P.E. Allaire, E.J. Gunter, Review: rotor balancing, *Shock and Vibration* 5 (1998) 325–336.
- [5] A. Muszynska, Rotor to stationary element rub-related vibration phenomena in rotating machinery—literature survey, *Shock and Vibration Digest* 21 (1989) 3–11.
- [6] S. Edwards, A.W. Lees, M.I. Friswell, Fault diagnosis of rotating machinery, *Shock and Vibration Digest* 30 (1998) 4–13.
- [7] C.B. Gibbons, Coupling misalignment forces, in: *Proceedings of the 15th Turbomachinery Symposium*, Gas Turbine Laboratory, College Station, Texas, 1976, pp. 111–116.
- [8] D.L. Dewell, L.D. Mitchell, Detection of a misaligned disk coupling using spectrum analysis, *Transactions of the American Society of Mechanical Engineers—Journal of Vibration Acoustics Stress and Reliability in Design* 106 (1984) 9–16.
- [9] F.F. Ehrich (Ed.), *Handbook of Rotordynamics*. McGraw-Hill, New York, 1992.
- [10] A.S. Sekhar, B.S. Prabhu, Effects of coupling misalignment on vibrations of rotating machinery, *Journal of Sound and Vibration* 185 (1995) 655–671.
- [11] G. Simon, Prediction of vibration behaviour of large turbo-machinery on elastic foundations due to unbalance and coupling misalignment, *Proceedings of the Institution of Mechanical Engineers, Part C—Journal of Mechanical Engineering Science* 206 (1992) 29–39.
- [12] M. Xu, R.D. Marangoni, Vibration analysis of a motor-flexible coupling-rotor system subjected to misalignment and unbalance, Part I: theoretical model and analysis, *Journal of Sound and Vibration* 176 (1994) 663–679.
- [13] M. Xu, R.D. Marangoni, Vibration analysis of a motor-flexible coupling-rotor system subjected to misalignment and unbalance, Part II: experimental validation, *Journal of Sound and Vibration* 176 (1994) 681–691.
- [14] B.J. Hamrock, *Fundamentals of Fluid Film Lubrication*, McGraw-Hill, New York, 1994.
- [15] A.W. Lees, I.C. Simpson, The dynamics of turbo-alternator foundations, in: *IMEchE Conference on Vibrations in Rotating Machinery*, Paper C6/83, London, UK, 1983, pp. 37–44.
- [16] A.W. Lees, The least squares method applied to identified rotor/foundation parameters, in: *IMEchE Conference on Vibrations in Rotating Machinery*, Paper C306/88, Edinburgh, UK, 1988, pp. 209–216.
- [17] G.A. Zanetta, Identification methods in the dynamics of turbogenerator rotors, in: *IMEchE Conference on Vibrations in Rotating Machinery*, Bath, Paper C432/092, 1992, pp. 173–181.
- [18] N.S. Feng, E.J. Hahn, Including foundation effects on the vibration behaviour of rotating machinery, *Mechanical Systems and Signal Processing* 9 (1995) 243–256.
- [19] A. Vania, *Estimating turbo-generator foundation parameters*. Politecnico di Milano, Dipartimento di Meccanica, Internal Report 9-96, 1996.
- [20] R. Provasi, G.A. Zanetta, A. Vania, The extended Kalman filter in the frequency domain for the identification of mechanical structures excited by sinusoidal multiple inputs, *Mechanical Systems and Signal Processing* 14 (2000) 327–341.
- [21] M.G. Smart, M.I. Friswell, A.W. Lees, Estimating turbogenerator foundation parameters—model selection and regularisation, *Proceedings of the Royal Society Series A* 456 (2000) 1583–1607.
- [22] J.K. Sinha, A.W. Lees, M.I. Friswell, R.K. Sinha, The estimation of foundation models of flexible machines, in: *Proceedings of Third International Conference—Identification in Engineering Systems*, Swansea, UK, 2002, pp. 300–309.
- [23] A.W. Lees, M.I. Friswell, The evaluation of rotor unbalance in flexibly mounted machines, *Journal of Sound and Vibration* 208 (1997) 671–683.
- [24] S. Edwards, A.W. Lees, M.I. Friswell, Experimental identification of excitation and support parameters of a flexible rotor-bearing-foundation system from a single run-down, *Journal of Sound and Vibration* 232 (2000) 963–992.
- [25] J.K. Sinha, A.W. Lees, M.I. Friswell, Estimating the unbalance of a rotating machine from a single run down, in: *Proceedings of 19th International Modal Analysis Conference*, Kissimmee, Florida, 2001, pp. 109–115.

- [26] J.K. Sinha, M.I. Friswell, A.W. Lees, The identification of the unbalance and the foundation model of a flexible rotating machine from a single run down, *Mechanical Systems and Signal Processing* 16 (2002) 255–271.
- [27] A.W. Lees, J.K. Sinha, M.I. Friswell, The identification of the unbalance of a flexible rotating machine from a single run-down, in: *Proceedings of the American Society of Mechanical Engineers Turbo Expo Conference*, Amsterdam, Netherlands, 2002, ASME paper GT-2002-30420.
- [28] M.A. Jordan, What are orbit plots, anyway? *Orbit*, December (1993) 8–15.
- [29] G.H. Golub, C.F. Van Loan, *Matrix Computations*, 3rd Edition, The John Hopkins University Press, Baltimore, MD, 1996.
- [30] P.C. Hansen, Regularisation tools: a MATLAB package for analysis and solution of discrete ill-posed problems, *Numerical Algorithms* 6 (1994) 1–35.
- [31] VSI Rotate User Manual, 2000. <http://www.vold.com>.
- [32] M.G. Smart, Identification of Flexible Turbogenerator Foundations, Ph.D. Thesis, University of Wales Swansea, Swansea, 1998.